Improved understanding of nitrate trends, eutrophication indicators and risk areas using machine learning

Deep S. Banerjee[1,2] and Jozef Skákala[1,2]

[1]Plymouth Marine Laboratory, PL1 3DH Plymouth, United Kingdom,
[2]National Centre for Earth Observation, PL1 3DH Plymouth, United Kingdom.

Correspondence: Deep S. Banerjee (dba@pml.ac.uk)

Abstract. Nitrate is an essential inorganic nutrient limiting phytoplankton growth in many marine environments. Eutrophication, often caused by nitrogen deposition, is a reoccurring problem in coastal regions, including the North-West European Shelf (NWES). Despite their importance, nitrate observations on the NWES are costly to obtain and thus sparse both in time and space. We demonstrate that machine learning (ML) can generate, from sparse observations, a skilled, gap-free, bi-decadal (1998-2020) surface nitrate data-set. We demonstrate that the effective resolution (scales on which the data-set is skilled) is slightly coarser than the 7 km and daily resolution of the product, but still completely sufficient to analyse nitrate dynamics on a monthly scale. With such a data-set we are able to demonstrate the following: (i) highlight the coastal regions that show strong Summer nutrient limitation, covering eutrophication-problem areas identified by the monitoring bodies (i.e. OSPAR), but also other regions, such as southern Irish coastline and parts of Irish Sea. Our results could indicate greater potential for eutrophication events in those regions subject to high riverine nutrient discharge scenarios. (ii) We demonstrate that bi-decadal 1998-2020 trends in coastal nitrate, responding to long-term policy-driven reduction in riverine discharge, are mostly modest with a notable exception of the Bay of Biscay. (iii) We show that winter nitrate plays relatively minor direct role in the phytoplankton bloom intensity the following spring, which can have some implications for using winter inorganic nitrogen as one of the eutrophication indicators (as often included by OSPAR). The last two results are consistent with recent findings in the literature (Axe et al., 2022; Devlin et al., 2023; Van Leeuwen et al., 2023). We propose to use the nitrate data-set for data assimilation and hypothesise that it has the potential to substantially improve phytoplankton forecast in the operational run.

1 Introduction

Nitrogen is one of the most important components of organic matter, needed for primary production in relatively large concentrations, as demonstrated by the Redfield ratios (Tett et al., 1985). Despite its large abundance (the Earth's atmosphere comprises 78% nitrogen as N_2), it is non-trivial to obtain nitrogen in forms useful for plants. As a consequence, nitrogen is often the most limiting nutrient for plant, or algae growth, including coastal marine environment (Ryther and Dunstan, 1971; Board et al., 2000). Nitrogen fixation, converting atmospheric nitrogen to forms useful for life, happens through various biotic and abiotic pathways, resulting in ammonium, nitrite and nitrate (Noxon, 1976; Hill et al., 1980; Postgate, 1998; Beman et al., 2008; Voss et al., 2013). Nitrate in the ocean is the primary nutrient for phytoplankton, with phytoplankton uptake enabling

nitrogen flows into higher trophic levels and various detrital and dissolved forms of organic matter. In a nitrogen-limited envi-

25 ronment, excess nitrate concentrations, primarily originating from agricultural runoff and industrial wastewater discharge, can stimulate harmful eutrophication events (Withers et al., 2014; Nazari-Sharabian et al., 2018). The thick layer of algae produced by these events may cut oxygen ventilation at the surface and after the algae die off and sink, the decomposers may consume vast amounts of oxygen, leading to marine hypoxia in the bottom part of the water column (Rabalais et al., 2002; Diaz and

30 Rosenberg, 2008). Furthermore, eutrophication events are often dominated by species that produce toxins (leading to harmful algae blooms, HABs) which have detrimental effects on the marine ecosystem by causing fish kills, seafood contamination, and even posing risks to human lives (Anderson et al., 2012). Additionally, high nitrate concentrations may lead under certain circumstances to excessive production of organic matter, which, upon decomposition, increases CO_2 concentration, contributing to ocean acidification (Doney et al., 2009). Eutrophication is a fundamental problem in many shelf sea and coastal areas

35 (Rabalais et al., 2009), where nitrate monitoring and predicting, along with other indicators (e.g. chlorophyll, dissolved oxygen, phytoplankton species), provides an essential tool informing marine management and policy.

An important region, subject to eutrophication, is the North-West European Shelf (NWES). The NWES is impacted by significant river inputs, such as Elbe, Rhine, Loire, Seine, Scheldt, Meuse, Humber, Weser or Thames which introduce substantial freshwater and nutrients into the region, influencing salinity and water properties (Sonesten et al., 2022). Open ocean shelf

40 exchange, especially transport of nutrients and carbon across the shelf break, plays another vital role in the NWES ecosystem dynamics (Huthnance et al., 2009). NWES has high ecological importance due to its high biological productivity, underpinning significant commercial fisheries and carbon sequestration (Pauly et al., 2002; Borges et al., 2006; Jahnke, 2010). Until the 1980s, the NWES, particularly near the German Bight and the Westerschelde estuary, experienced notable shifts in nutrient distribution, primarily driven by increased continental nutrient inputs. Riverine discharges, particularly from the Rhine and

45 Elbe, have been identified as major contributors to nutrient dynamics in the region (Brockmann and Eberlein, 1986; Radach, 1992), having adverse effects on the local ecosystem. However, EU regulations following the OSPAR convention in 1992 substantially decreased the nitrate deposition into the NWES (Soetaert et al., 2006; Radach and Pätsch, 2007; Lenhart et al., 2010a; Burson et al., 2016a; Axe et al., 2022; Sonesten et al., 2022).

The NWES nitrate concentrations are operationally simulated and predicted (Skákala et al., 2018), however, the NWES

50 nitrate observations are too sparse to properly constrain the simulated nitrate through data assimilation. There is existing work on developing statistical algorithms to derive nitrate from satellite (Durairaj et al., 2015; Chen et al., 2023), but these have so far been developed either for the global open ocean, or for other regions than NWES (such as different regions in Asia, or California, Yu et al. (2021); Chen et al. (2023)), and those algorithms are unlikely to work for NWES. The current operational NWES system is mainly constrained by the much more robust satellite temperature and chlorophyll observations (Skákala et al.,

55 2018, 2021, 2022) and avoids assimilating nutrients entirely. Furthermore, due to its univariate nature, the operational system fails to directly constrain most of the non-assimilated variables including nutrients. Consequently, the nitrate reanalyses and forecasts produced by the operational system are known to have substantial biases, inherited from the model free run (Skákala et al., 2018, 2022). Although the simulated physics and chlorophyll from the reanalysis validate well against observations (Skákala et al., 2018, 2022), the nitrate NWES product is of more limited use.

In this work we develop and validate a new bi-decadal NWES nitrate product derived from the available observations using advanced machine learning (ML) algorithms. The nitrate product is developed for the ocean surface, where nutrients have the potential to most significantly drive phytoplankton growth. This is to our knowledge by far the most complete and detailed observation-based sea surface nitrate data-set on the NWES. Unlike the NWES operational reanalysis, the data-set validates skillfully against the independent observations. Using our NWES nitrate product we are able to discuss several important topics, like the impact of winter nitrate pre-conditioning on the inter-annual phytoplankton variability, what are the most nutrient-limited coastal NWES geographic areas and what are the trends in nitrate concentrations on the NWES. To do so, we maximise our reliance on the observational data and use ML and modelling to effectively fill the large data-gaps, either through statistics, or dynamical consistency imposed by deterministic modelling.

2   Methodology

2.1   The ML model

We used as the ML model a Feed-forward Neural Network (NN) designed through the Autokeras library using a Structured Data Regressor (Jin et al., 2019). This approach streamlined the process of hyperparameter optimization and model architecture discovery through an automated procedure, significantly reducing the need for manual intervention. The routine follows an iterative trial-and-error approach by looping through several possible combinations of various hyperparameters, such as learning rate, optimizers, and the number of dense layers with different combinations of nodes. It then selects the best model architecture with the highest skill score against the validation dataset and saves it for final prediction against the test data.

The final model architecture comprised several layers (see Fig.S1 of Supporting Information, SI): (i) the input layer with 25 nodes corresponds to the input features or predictors, (ii) a multi-category encoding layer, encoding categorical features (i.e., month and day of the year) into a numeric form that can be understood by the network, (iii) a normalization layer, which normalizes the input data to improve model training by facilitating improved model convergence time and better performance, avoiding dominance of features with larger magnitudes, and providing better stability, (iv) two dense layers with 128 and 256 nodes, respectively, with each of these layers being followed by a Rectified Linear Unit (ReLU) activation function to introduce non-linearity into the model, (v) dropout layer applied to prevent overfitting by randomly dropping out a fraction of neurons during the training phase, and (vi) regression head with a single node that produces the final prediction, i.e., nutrient concentration. During the training phase, the model's performance was evaluated using standard metrics, i.e., Mean Squared Error (MSE), and then estimating relative error with respect to the validation dataset.

2.2   Data

2.2.1   The input features

To avoid biases towards operational models, the NN model input features were selected to be either observational data, or reanalyses of variables closely constrained by the observations. One of the main challenges in building ML for environmental

applications is to combine (often sparse) data with typically inconsistent domains of coverage across a various spatial and temporal scales. The most robust NWES-focused observational data-sets are obtained through satellite optical measurements. For physics these are data such as sea surface temperature (SST), or altimetry. For biogeochemistry the most typical derived data-set is surface chlorophyll a concentration obtained from the ocean color (OC). Recently, new remote-sensing algorithms were developed to partition the total chlorophyll concentration into phytoplankton functional types (PFTs) based largely on phytoplankton size-classes (Brewin et al., 2010, 2017), and PFT chlorophyll products are now operationally assimilated into the NWES model (Skákala et al., 2018). The reanalyses from the NWES operational model have been found to have a very close match-ups with the assimilated observations (Skákala et al., 2018, 2022), and act as natural extensions of the observations, forming a complete data-set on a gridded domain. We have extracted a range of NN model features from a NWES physical-biogeochemistry reanalysis products NWSHELF_MULTIYEAR_BGC_004_011 and NWSHELF_MULTIYEAR-_-PHY-_004_009 (downloadable from the EU Copernicus portal, https://marine.copernicus.eu/, see also Kay et al. (2016)), covering the 1998-2020 period with daily and 7 km spatial resolution. The product is based on assimilating satellite SST, temperature and salinity profiles, as well as OC PFT chlorophyll, into the operational Nucleus for Ocean Modelling (NEMO, Madec et al. (2017)) model, coupled through Framework for Aquatic Biogeochemical Models (FABM, Bruggeman and Bolding (2014)) to the biogeochemistry, European Regional Seas Ecosystem Model (ERSEM, Baretta et al. (1995); Butenschön et al. (2016)). The extracted features were for (i) SST, (ii) chlorophyll ocean surface concentrations from four PFTs, which were assimilated into the NEMO-FABM-ERSEM model (diatoms, microphytoplankton, nanophytoplankton and picophytoplankton), as well as for (iii) total surface phytoplankton carbon, (iv) total surface chlorophyll and (v) total surface net primary production. Although these features were selected from the reanalysis, they either correspond to the assimilated variables (SST, PFT chlorophyll), or to variables which are dynamically very close to the assimilated PFT chlorophyll (phytoplankton carbon, net primary production) and therefore well constrained by the assimilation. Additionally, we also included SST observations from the Global Ocean OSTIA product (Good et al., 2020; Donlon et al., 2012) in the input feature dataset. Interestingly our tests (not shown here) indicated that the NN model did not perform as well without this additional SST data-set, so both sources of SST information (reanalysis and OSTIA) were used.

We have also used input features describing riverine discharge into the ocean. These included riverine discharge data for oxygen and nutrient loads (i.e., nitrate, phosphate, silicate, ammonia, and oxygen) at all relevant river mouths in the NWES domain. Daily time series of river discharge are used for 1998-2017. From 2018 only climatologies were available and were used for the remaining 2018-2020 period. The daily riverine data were obtained from an updated version of the river dataset from Lenhart et al. (2010b). Climatology of daily discharge data were taken from the Global River Discharge Data Base and the Centre for Ecology and Hydrology (Young and Holt, 2007). Unlike a hydrodynamic model, a NN does not follow any advection mechanism or transport to carry the effect of river discharge over space and time. To account for advection the NN model would have to ideally include time-lagged riverine inputs, where the time-lag would increase with the spatial distance from the river mouth. This would hugely increase the complexity of the NN model. In this work we have decided to opt for less complex models and avoid using time-lagged NN inputs. To consider nearly-instantaneous riverine effect in a simplified way, we have distributed the riverine discharge data around the river discharge point sources. This was done by spatially extrapolating all the
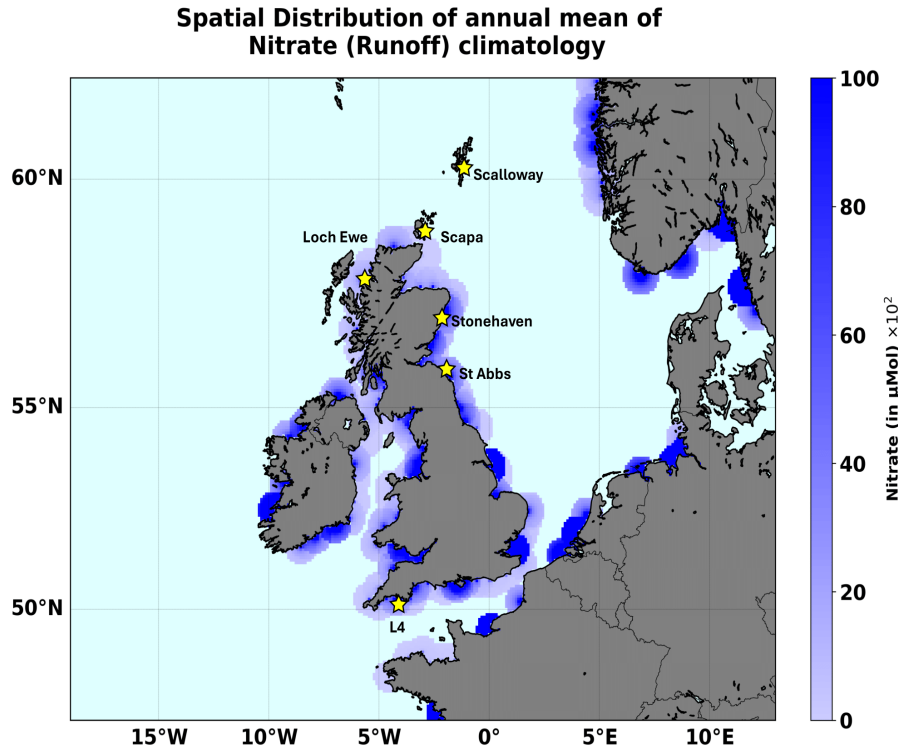
Figure 1. The areas with river input on the NWES domain. We mark the location of the stations providing the test data for this study: L4 and the five Scottish coastal stations.

runoff variables at all the daily discharge points over a 50 km circular radius surrounding the main discharge point, by making the inputs decay inversely from the maximum at the center to a zero value at the edge (see Fig.1). However, such scheme is clearly a major simplification for the real river impact (e.g. Painting et al. (2013); Lenhart and Große (2018)) and should be ideally improved upon in the future work.

130   Another data-set that was used as input features into the NN model was the ERA-5 atmospheric reanalysis (Hersbach et al., 2020), which has a horizontal resolution of 0.25°. The input feature dataset includes variables such as downwelling shortwave radiation at the ocean surface, specific humidity, temperature at 2m above the ocean surface, sea level pressure, total precipitation, and zonal and meridional wind components at 10m above the ocean surface. These near-surface atmospheric drivers play a crucial role in governing and redistributing surface nitrate through air-sea interactions and atmospheric deposition

135   of nitrogen, which accounts for one-third of the non-recycled nitrogen supply in the ocean and up to around 3% of annual new biological production (Duce et al., 2008). The atmospheric data, however, did not include any direct products for atmospheric nitrogen deposition. Finally, we used structural temporal and geographic data, i.e. the time of the year (month, day), latitude,

longitude, depth and bathymetry as input features. This type of information enables the model to learn the geographic patterns in nitrate, including its seasonal climatology, substantially enhancing its predictive accuracy.

140 All the input features were considered at the same times as the predicted nitrate. The input features importance was ranked in the SHAP (Shappley Additive exPlanations) analysis, presented in Fig.S2 of the Supporting Information (SI). The SHAP analysis indicates that the structural input features are among the most important, followed by some atmospheric and oceanic physics features (incoming short-wave radiation, SST), which can partly account for seasonal climatology as well. Specific riverine discharge input features (e.g. of nitrate itself) are highly important too (Fig.S2 of SI), with a range of biogeochemical

145 variables (total surface chlorophyll, total surface net primary production and total surface carbon) being around the middle of the importance ranking. As already mentioned, we have tested also versions of the NN model with a reduced number of input features (e.g. removing the less important features from the SHAP analysis), but the model performance became slightly worse compared to the previous one.

2.2.2 The predicted nitrate data, the training and the validation process

150 The 1998-2018 nitrate observations were obtained from the International Council for the Exploration of the Sea (ICES) Dataportal (*https://www.ices.dk*). The extracted dataset spans a geographical range from 19W to 10E in longitude and from 47N to 62N in latitude, ensuring wide representation of the dynamics and variability of the NWES region. The ICES data were obtained from a wide range of in situ measurements, e.g. by cruises, floats, moorings, or buoys. In the training and validation process, the ML model inputs were linearly interpolated into the ICES data locations, and then the ICES data from the 1998-

155 2015 period, containing 43572 relevant data-points, were used for training and validation of the NN model (with 80% data used for training and 20% used for validation). Finally, the 2016-2018 ICES data, containing 2984 data-points, were used as test data. The spatial coverage of all the ICES training, validation and test data is shown in Fig.2.

  Several other observations were used as test data, to demonstrate the ML model skill: (i) nitrate data from the L4 station, which is operated by the Western Channel Observatory (https://www.westernchannelobservatory.org.uk/) and is located

160 in the western English Channel approximately 13 km from the Plymouth Sound, providing one of the longest continuous ecological time-series in the world (Harris, 2010). The L4 nitrate data-set covered the whole 1998-2020 period, and despite several data-gaps, during most of this period it was sampled approximately with 5-7 day frequency. (ii) Another independent nitrate test data were obtained from The Scottish Coastal Observatory Dataset (https://data.marine.gov.scot/dataset/scottish--coastal-observatory-dataset-1997—2020, see also Bresnan et al. (2016); Hindson et al. (2018)), covering five locations near

165 the coastline of Scotland (Loch Ewe, Scalloway, Scapa, St.Abbs, Stonehaven), providing time-series of differing lengths: from the longest, covering the 2008-2020 period (Scapa, Scalloway), to the shortest, covering the 2017-2020 period (St.Abbs). The measurements at those stations had typically 5-7 day frequency. The locations of the L4 and the five Scottish Stations are all marked in Fig.1. It should be noted that none of the L4 data and the data from the Scottish stations were included in the ICES data-set.

170 Finally, after validating the NN model, we have run it for the full 1998-2020 period across the whole Copernicus NWES reanalysis domain (see Fig.3), taking Copernicus reanalysis, river and ERA-5 atmospheric forcing inputs (both interpolated
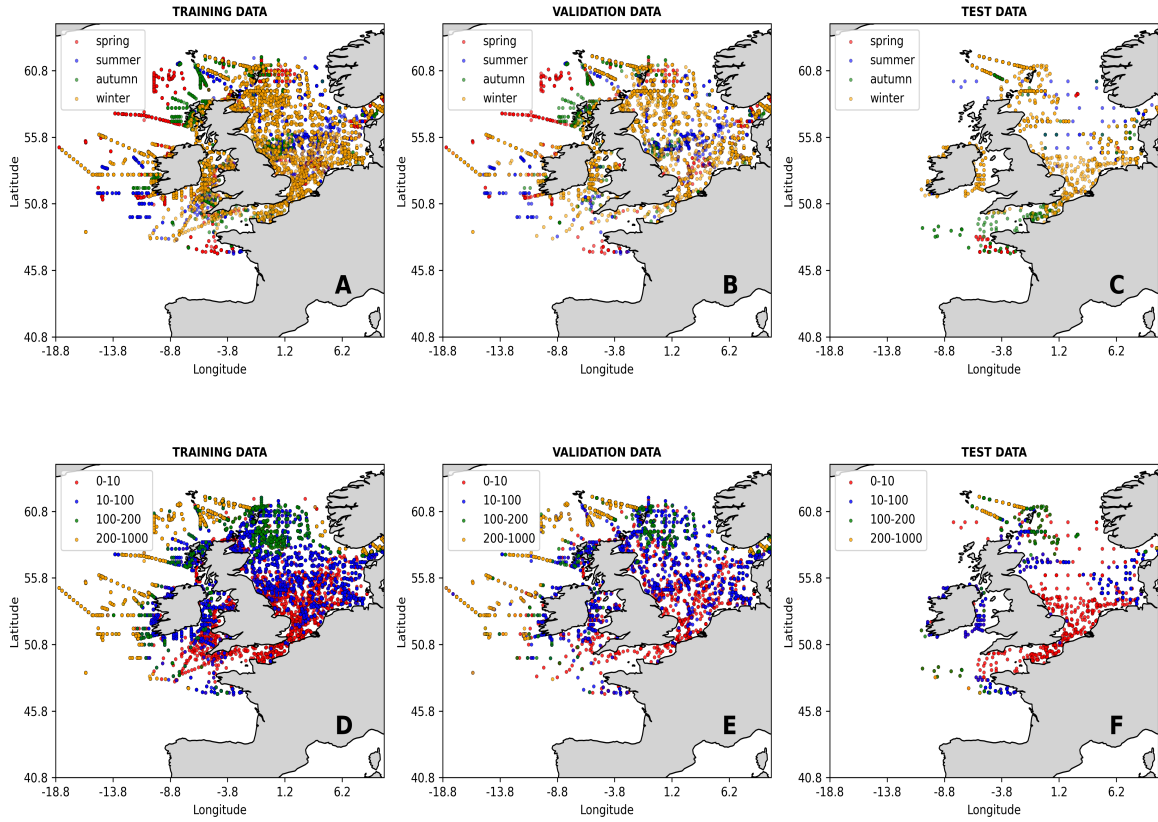
Figure 2. The locations of the ICES data used in this study split into training, validation and test data. The data-points are colored with respect to season when the measurement was taken (upper row) and by the depth range (in m) at which the measurement was taken (bottom row).

into the Copernicus reanalysis domain) and producing a gap-free bi-decadal, daily, 7 km resolution reconstruction of nitrate. This final data-set underpins the results from this study.

2.3 Skill metrics

We used the Relative Performance (RP) skill metric to compare the performance of the NN model from this study with the reanalysis:

$$RP(NN, Rean) = 100 \cdot \frac{(|NN - Obs| - |Rean - Obs|)}{Obs}. \tag{1}$$

In Eq.1 "Obs" stands for observations, "NN" for predicted values by the NN model and "Rean" for reanalysis. Negative values of the RP metrics from Eq.1 indicate that NN model outperforms reanalysis and vice versa.

180   The bias between any model "Mod" ("Mod" could be either NN, or reanalysis) and observations is defined as

$$\text{Bias(Mod, Obs)} = \langle \text{Mod} - \text{Obs} \rangle, \tag{2}$$

where the averaging $\langle ... \rangle$ is taken through all the available, matching, model and observational data.

The Bias-Corrected RMSE (BC-RMSE) is defined as RMSE after the bias h as been subtracted from the model:

$$\text{BC-RMSE} = \sqrt{\langle (\text{Mod} - \text{Obs} - \text{Bias})^2 \rangle}. \tag{3}$$

185   Apart from the metrics from Eq.1-3, we have also used Pearson correlation. Our tests have shown that the effective temporal resolution of the NN model (time-scale on which it performed best relative to the test data) is around 15 days (the tests are not shown here, but some insight is provided by Fig.S3 of SI). We have therefore low-pass filtered all the compared data on a 15-day scale, before any of the metrics from this section was applied.

3   Results and discussion

190   ### 3.1   Model validation

Fig.4, Tab.1 and Fig.S4-S5 of SI demonstrate that the NN model shows a very good skill relative to the test data from ICES, L4 and the Scottish stations, and substantially outperforms the existing Copernicus reanalysis product for NWES nitrate. For example the bias measured by the ICES test data has been reduced by more than 80% relative to the reanalysis, the BC-RMSE has been reduced by more than 60% and the Pearson correlation has increased from 0.27 to 0.72. Comparison to the data

195   from coastal stations shows less consistent improvement in terms of bias relative to the reanalysis, but the NN model still outperforms the reanalysis in BC-RMSE and R at each of the locations.

Because the nitrate time series are dominated by the seasonal signal, it is important to explore whether the model skill extends beyond predicting the local nitrate seasonal (e.g. monthly) climatology. This is much harder to validate, as one needs long term time-series at specific locations, which are rare. We have looked at the data from the L4 station and five Scottish

200   locations to analyse the ML model skill to capture interannual variability of nitrate. The results (shown in Tab.1 and Fig.S3 of SI) are more mixed: at L4 station, which has from all the locations the longest time-record and richest data-set, the ML model performs very well in predicting the inter-annual nitrate time-series. It is interesting that at the same location the reanalysis does a very poor job in doing the same (Tab.1). At Scottish stations the ML model correctly captures the size of the interannual variability in nitrate, but it struggles to capture the variability itself (the R metrics in Tab.1). It is however noteworthy that some

205   of the time-series at the Scottish locations are relatively short (see Sec.2.1) and therefore not the most suitable for this type of analysis.

Finally, the test data selected from the ICES data-set are time-separated from the training and validation data, but were spatially located in largely overlapping regions (see Fig.2). It is therefore important to explore the possibility that, due to geographic proximity, some ML skill has been transferred from the training/validation data to the test data. This is done in

210   Fig.S6 of SI, showing how the skill evolves as a function of spatial separation between the test data and the training/validation
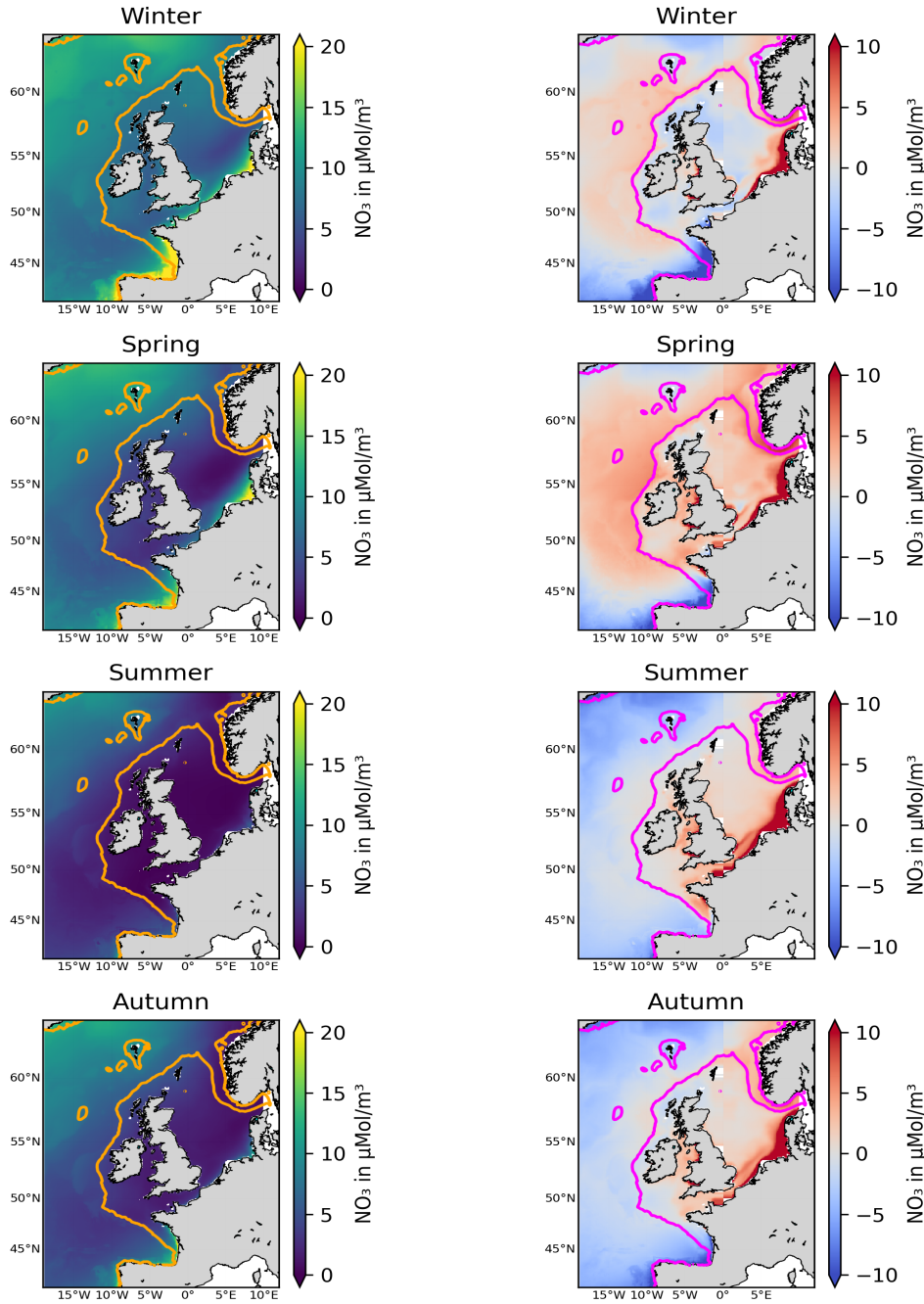
Figure 3. The left-hand panels show the NN-reconstructed 1998-2020 average surface nitrate concentrations for different seasons (corresponding to dominant mode of temporal variability in nitrate). The right-hand panels show the same averages for the relative bias of the Copernicus surface nitrate reanalysis (Kay et al., 2016) with respect to the NN-reconstructed data-set (reanalysis minus NN-reconstructed). The contours mark NWES (bathymetry < 200 m).
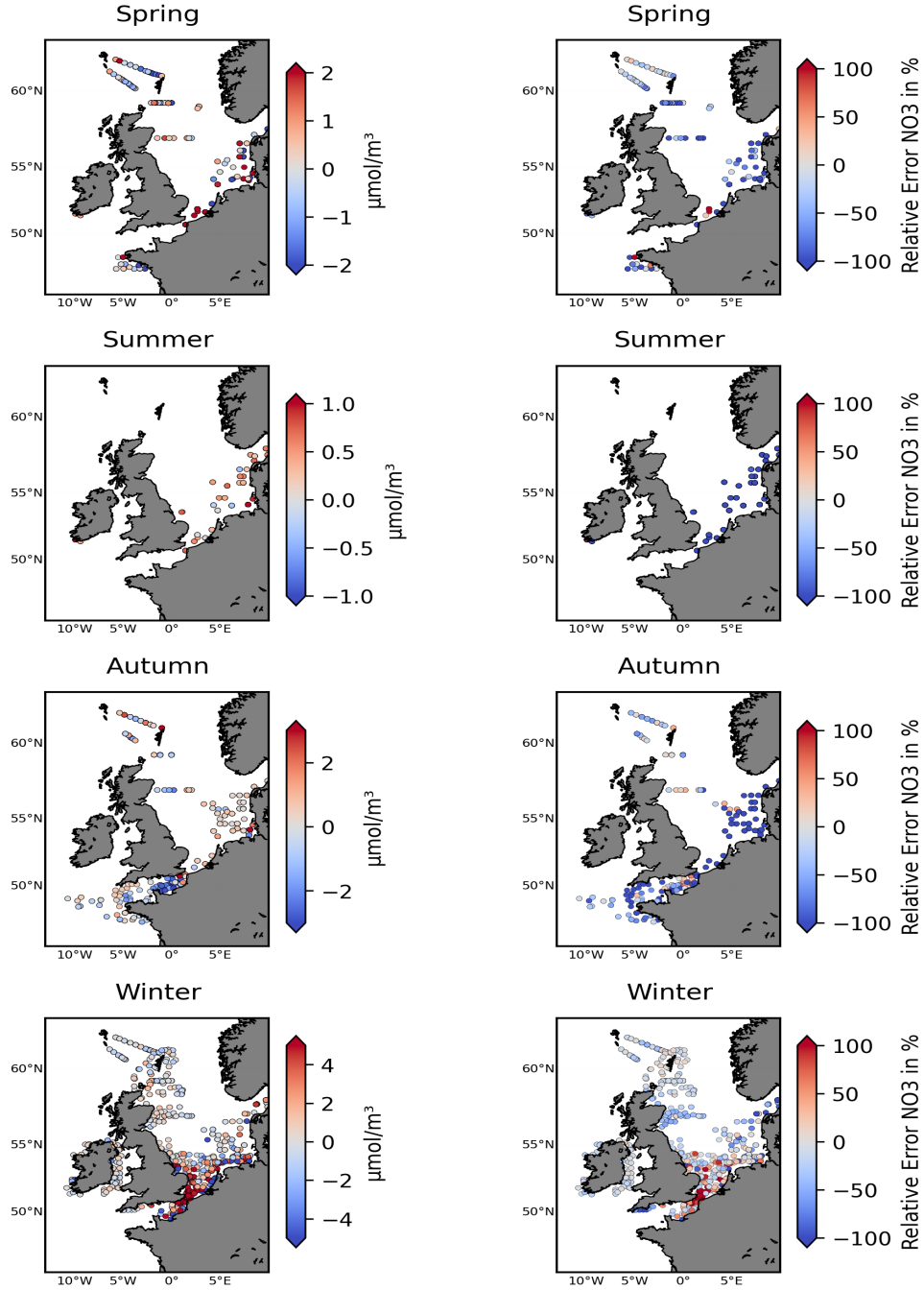
Figure 4. The left-hand panels show the ICES nitrate test data locations for different seasons, with the colorbar accounting for the NN-model skill (difference between predicted and observed nitrate: predicted - observed). The right-hand panels show the Relative Performance metrics between the NN model and the Copernicus reanalysis skill, as defined in Eq.1. It marks an NN-model improvement (blue), or degradation (red) relative to the reanalysis, when compared (in %) to the observed nitrate concentrations.

Table 1. The skill of the NN model in predicting nitrate compared with the Copernicus reanalysis (Kay et al., 2016). Skill is measured by bias (Eq.2, in μmol/m^3), Bias-Corrected Root Mean Squared Error (BC-RMSE, Eq.3, in μmol/m^3) and Pearson correlation (R). The rows represent different test data from ICES and the coastal stations. The last two rows show the skill of the NN model and the reanalysis to predict interannual, low-pass filtered time-series (for details see Fig.S3 of SI). For the five Scottish stations we show only the averaged result through all the stations.

Test data	NN predicted			Reanalysis		
	bias	BC-RMSE	R	bias	BC-RMSE	R
ICES	0.62	2.37	0.72	3.18	6.15	0.27
L4	-1.03	1.85	0.79	0.20	2.22	0.72
Scalloway	0.98	2.1	0.8	1.08	2.76	0.64
St.Abbs	-0.25	1.25	0.9	0.73	1.87	0.85
Scapa	1.52	1.52	0.86	0.33	2.13	0.69
Stonehaven	-0.53	0.97	0.95	0.09	2.04	0.78
Loch Ewe	1.57	0.92	0.93	0.57	1.1	0.89
L4 interannual	–	0.72	0.52	–	0.99	0.08
Scottish interannual	–	0.512	-0.144	–	0.756	0.204

data. Although there is large variability in the skill, Fig.S6 shows no significant trend with spatial distance, indicating that the ML model skill does not decrease (even slightly improves) with the increase in spatial separation.

3.2 The bi-decadal nitrate product, the trends, variability and implications

Fig.3 shows the 1998-2020 seasonally averaged NWES nitrate concentrations. It is clear from the spatial nitrate distributions that the NN model does not capture sufficiently the $\sim$ 7 km scale variability, including the exact NWES boundaries, but it does reasonably capture coarse resolution nitrate distributions (see Fig.5 for comparison with the World Ocean Atlas, WOA, product of Garcia et al. (2019)). Similarly, our analyses (including Fig.S3-S5 of SI) suggest that the effective temporal resolution of the NN product is $\sim$15-day, rather than daily. Fig.3 also provides seasonal comparison with the Copernicus reanalysis product, evaluating the significant reanalysis biases throughout the 1998-2020 period. The Copernicus reanalysis validation gives similar results to validation from Kay et al. (2016), who compared the reanalysis with the North Sea Biogeochemical 1960-2014 Climatology (Hinrichs et al., 2017).

The winter nitrate concentrations play an important role in pre-conditioning of the spring bloom, which largely drives the NWES biogeochemical seasonal cycles (Huisman et al., 1999; He et al., 2011). The winter dissolved inorganic nitrogen is used by OSPAR (in combination with other parameters) in its Common Procedure (OSPAR, 2005), as an important indicator for NWES eutrophication and next season's growth (Axe et al., 2017; Topcu and Brockmann, 2021). The hypothesis, that the intensity of the spring phytoplankton bloom is directly related to the abundance of nutrients in the winter before the bloom, has been investigated here through nitrate.
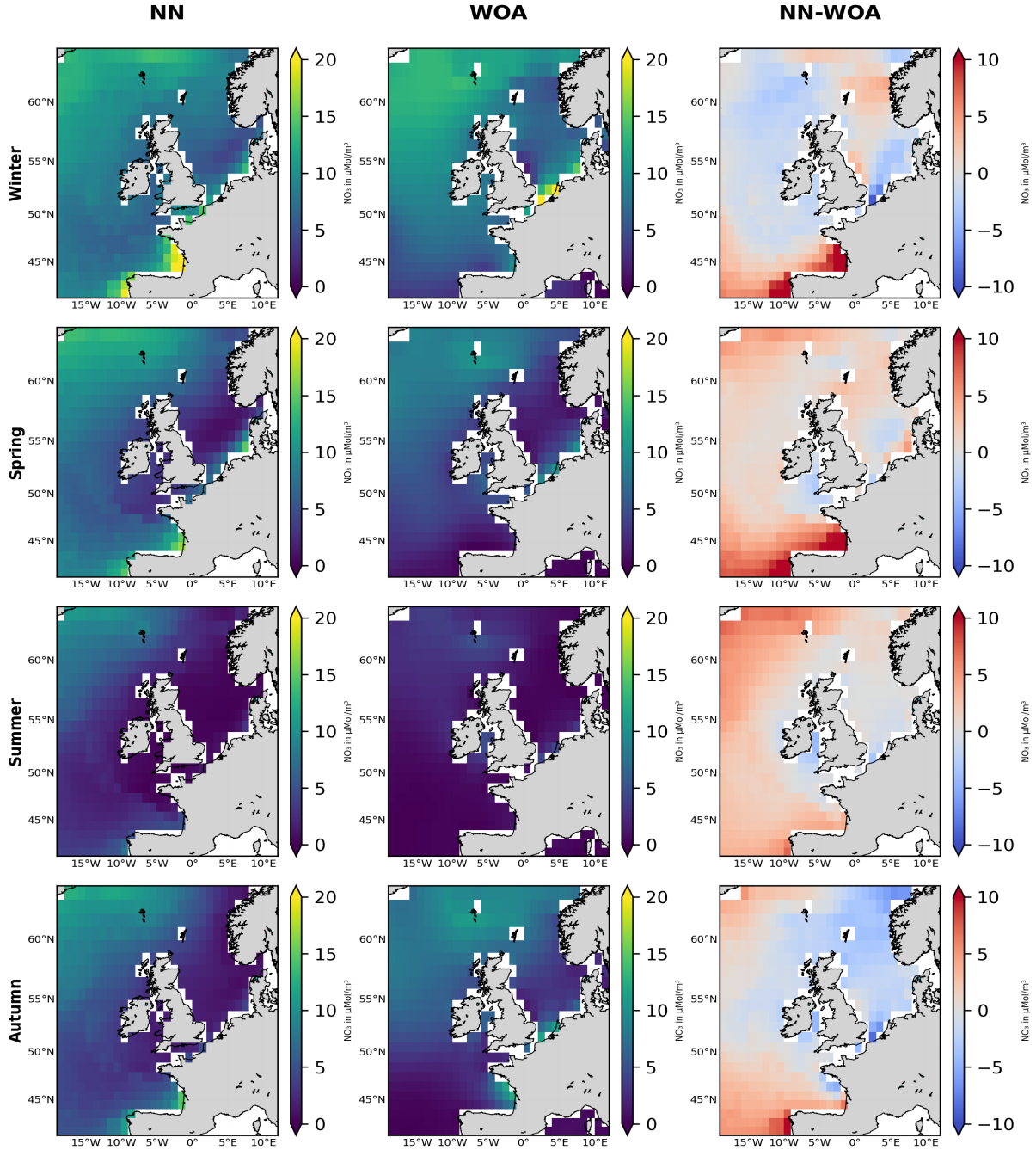
Figure 5. Seasonal comparison of the NN-predicted 1998-2020 surface nitrate averages (left-hand panels) with the World Ocean Atlas 2018 (WOA) product (middle panels, Garcia et al. (2019)). Right-hand panels show the difference (NN-predicted minus WOA product) for corresponding seasons. The NN-predicted data are coarse-grained on the WOA 0.25° spatial resolution scale. The focus is on spatial nitrate features, rather than nitrate concentration values, as the WOA atlas averages data for the whole 1900-2018 period, including highly eutrophic decades in the 1970's and 1980's.

In Fig.6:A we have found only limited evidence for the relationship between the winter (December - February) nitrate and spring bloom intensity, i.e. statistically significant positive Pearson correlation has been found only in the western English Channel region, near the shelf-break in the Celtic Sea, around the Bay of Biscay and in the south-west of the model domain (accounting at most for 30-35% of explained variance). Fig.6:A also shows that these are regions where the inter-annual nitrate variability appears to be relatively large (>5% of the winter average in the majority of the region, with 10-20% in specific sections, Fig.6:B) and therefore capable to reveal stronger relationship with spring chlorophyll. For most of the domain, there is lack of clear correlation between inter-annual winter nitrate and spring chlorophyll, which could be explained by the fact that both are driven by the interannual variability in the atmosphere (Dutkiewicz et al., 2001; Follows and Dutkiewicz, 2001; Ueyama and Monger, 2005; Henson et al., 2006; Zhai et al., 2013). Increased winds can lead to more mixing and elevated surface nutrients, whilst dampening blooms by transporting phytoplankton below the Sverdrup critical depth, as proposed by popular hypotheses explaining the North Atlantic spring blooms (Sverdrup, 1953; Huisman et al., 1999). Furthermore, there is lack of complete agreement on what are the dominant drivers of the spring bloom in the North Atlantic, and arguments have been raised supporting the view that blooms result much more from the internal ecosystem dynamics (e.g. zooplankton control over phytoplankton, Behrenfeld and Boss (2014)), compared to what was assumed by the traditional hypotheses focusing on physics. It is noteworthy that the weak link between winter nitrate and phytoplankton growth reported here is also consistent with recent results by Van Leeuwen et al. (2023).

In Fig.6:C we look at correlations between inter-annual time-series of summer nitrate and chlorophyll concentrations. High positive correlation in Fig.6:C indicates regions where growth is either strongly nitrate-limited, or limited by other driver positively correlated with nitrate. Realistically the only such drivers can be other nutrients, i.e. phosphate (there is substantial phosphate-limitation on NWES, Skogen et al. (2004); Philippart et al. (2007); Loebl et al. (2009); Lenhart et al. (2010a); Burson et al. (2016b); Grosse et al. (2017)), so we can conclude that those regions are strongly nutrient-limited in the Summer (with the nutrient being likely nitrate). The coastal part of the regions with strong positive correlation delimits areas which could be more sensitive than others to high river nutrient loads. This does not automatically imply high risk of eutrophication, as this would also depend on other factors, such as the overall river outflow in each area and the socio-economic activity, but it indicates certain increased vulnerability. The Fig.6:C shows high Summer nitrate-chlorophyll positive correlations mostly in the southern North Sea region, in the western English Channel, Bay of Biscay and the south-west of the domain. These are again the regions where the inter-annual fluctuations of summer nitrate are relatively large (Fig.6:D). Interestingly, the eutrophication-problem areas, as identified by the OSPAR NWES eutrophication status reports (such as south-eastern North Sea, coastal areas around Brittany, Axe et al. (2017); Devlin et al. (2023)), fall under these vulnerable zones delimited in Fig.6:C. However, Fig.6:C includes also other regions, such as eastern coastline of Scotland, southern coast of Ireland and zones in the Irish Sea.

Finally Fig.7, shows 1998-2020 trends in winter nitrate concentration over the NWES domain. In most of the domain no statistically significant nitrate trends have been detected, but some small negative trends ($\sim 0.02\ \mu$mol.m^{-3}.year^{-1}) were found in the Southern North Sea and the north-east region near the Norwegian trench. Somewhat larger ($\sim 0.08\ \mu$mol.m^{-3}.year^{-1}) statistically significant negative trends have been found in specific locations of the Bay of Biscay. These results (e.g. from the
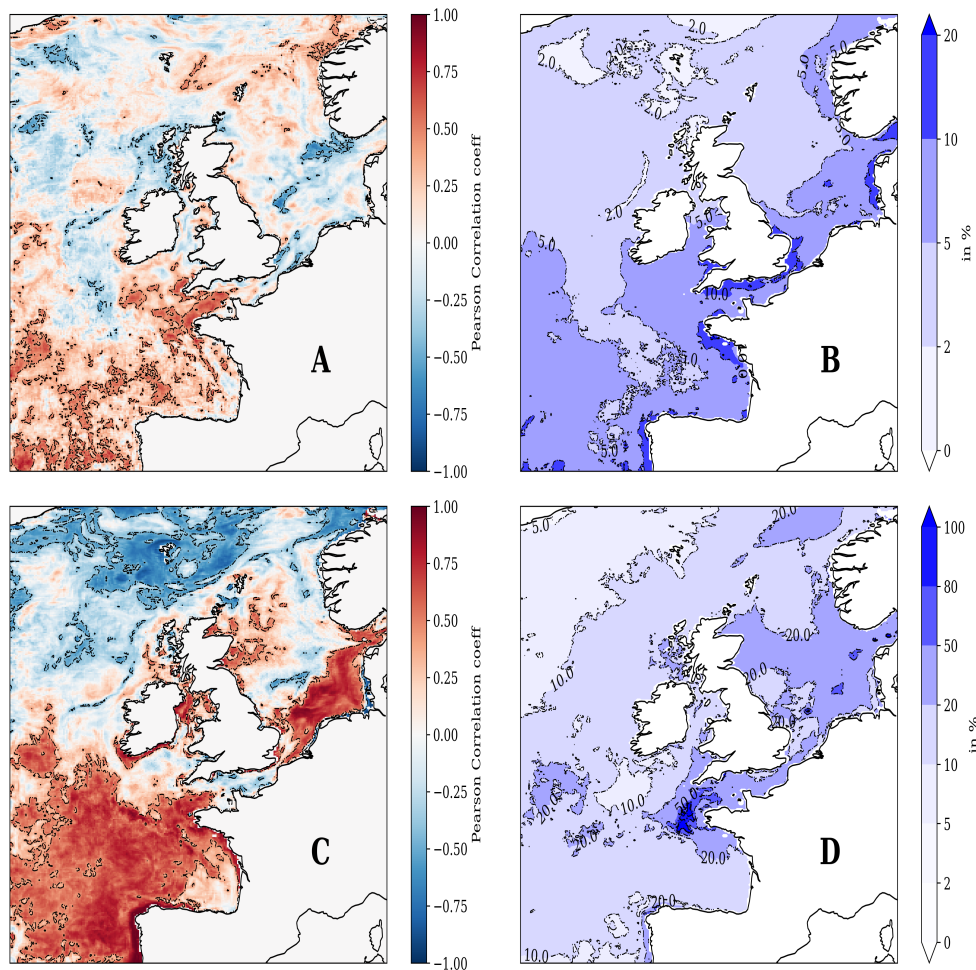
Figure 6. The upper left-hand panel (A) shows the Pearson correlation between the NN-predicted mean winter surface nitrate concentrations and the mean (following) spring surface chlorophyll concentration from the Copernicus reanalysis. The upper right-hand panel (B) shows the inter-annual variability for NN-predicted winter surface nitrate concentration (for 1998-2020, measured by the standard deviation), relative to the 1998-2020 winter mean (in %). The bottom left panel (C) is similar to panel A, but showing the Pearson correlation between the NN-predicted summer surface nitrate concentration and the summer surface total chlorophyll concentration from the Copernicus reanalysis. The panel D is the same as the panel B, but showing inter-annual variability of NN-predicted surface nitrate concentration in the summer, rather than winter. The dashed contours in panels A and C show regions where the correlation is statistically significant (p-value < 0.05).
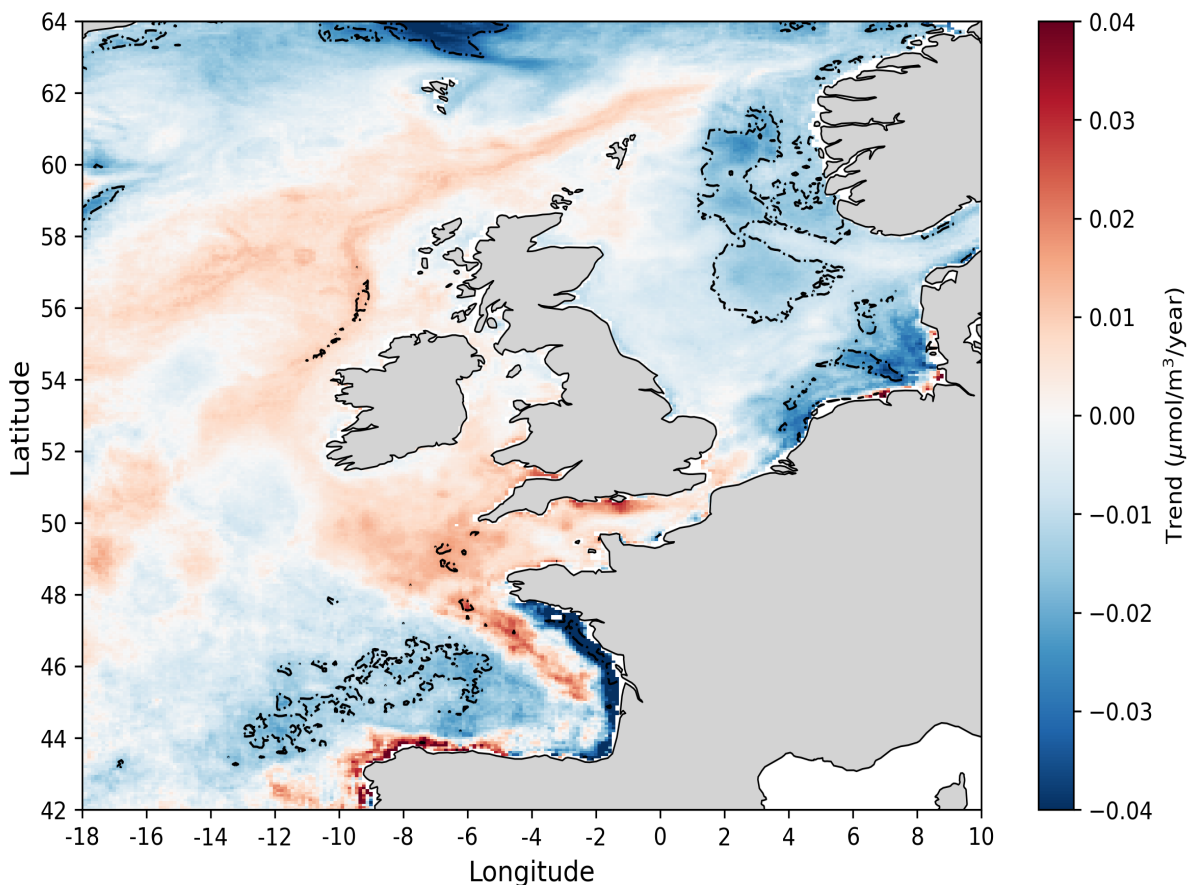
Figure 7. Linear trends at each spatial location in the annual nitrate concentration 1998-2020 time-series obtained from the NN model prediction. Dashed contours mark areas with statistically significant trends (p-value < 0.05).

Southern North Sea) are broadly consistent with what has been reported for this period in the recent OSPAR report (e.g. Axe et al. (2017, 2022)). These small trends may follow the smaller rates of reduction in the nitrate riverine inputs during the data period (1998-2020), compared to their large reduction in the 1980's and earlier 1990's (Duarte, 2009; Brockmann et al., 2018; Greenwood et al., 2019). It should be however noted that significant reduction in atmospheric nitrogen input has been reported in the last decades (Devlin et al., 2023).

4 Conclusions

In this work we have demonstrated that, using sparse observations across the North-West European Shelf (NWES), machine learning (ML) can provide a powerful tool to reconstruct a spatially complete sea surface nitrate data-set over period of 23 years. We have shown that the data-set has substantially better match-ups with independent test data than the existing NWES nitrate reanalysis. Using the newly developed product, we have identified nutrient-limited coastal areas with potentially strong ecosystem responses to an event of river nutrient pollution, addressed nitrate decadal trends, and tested how successfully winter nitrate can be used as a predictor of the phytoplankton spring bloom. The areas of strong ecosystem response to nutrient loads were identified as south-east of the North Sea, coastline of Brittany and the bay of Biscay (areas previously marked by OSPAR as eutrophication-problem, Axe et al. (2017); Devlin et al. (2023)), but also additional coastal areas were identified in the south of Ireland, eastern Scottish coastline and the Irish Sea. We have found that nitrate trends in the last two decades were mostly minor, with the exception of the coastline in Bay of Biscay. This confirms recent observations by Axe et al. (2017, 2022); Devlin et al. (2023). We have also demonstrated that winter nitrate is only a limited predictor of the growth next season, which again supports recent findings of Van Leeuwen et al. (2023).

There are many other potential scientific uses of the nitrate data-set, e.g. we propose to assimilate the nitrate data into the NWES operational model, correcting the model significant nitrate biases, potentially improving its dynamics and its short-range forecasts. The model skill in simulating phytoplankton is known to quickly degrade with the forecast lead time (e.g. Kay et al. (2016); Skákala et al. (2018)) and biases in nitrate might be one of the leading factors in driving this. Assimilation of nitrate products derived here will be addressed in the near future.

Several extensions of this work would be also desirable, such as utilizing ICES data for other biogeochemical indicators to produce ML-informed multi-variate data-sets across the whole NWES domain (these should include other nutrients and oxygen). ML could also identify valuable patterns of relationships across the multiple variables. Furthermore, the model developed here did not show very good skill in capturing high-frequency (daily) temporal variability, including extreme events. This might be due to processes providing ocean with memory significantly longer than the daily time-scale of the product. Representing ocean memory by the NN model might require using time-lagged input features, which could substantially inflate the size and the complexity of the model. Despite that, including such features into the NN model should be considered in the future, i.e. also with respect to developing a more realistic river discharge advection scheme, than the one used here, which is a major challenge. Curiously the finer spatio-temporal representation of nitrate could be automatically improved if we assimilated the NN-predicted nitrate into the dynamical model, as such scheme would benefit from both, the dynamical model advection scheme and the improved representation of the (coarser resolution) nitrate by the NN model. Other future activities should include re-training the NN model, whenever newer and potentially better observational products appear for its inputs (such as new riverine discharge data appearing in the last years, van Leeuwen and Lenhart (2021)). Finally, ML tools designed to specifically capture extreme phenomena can be deployed in the future and extend the applicability of this work.

Code and data availability. The ML software is placed in https://github.com/neccton-algo/nn-bgc. We used in this study the atmospheric ERA-5 product of the European Centre for Medium-range Weather Forecasting (ECMWF, https://www.ecmwf.int/), as well as river data that are stored on MonSOON HPC and can be obtained upon request. We have also used EU Copernicus reanalyses; the NWSHELF_-MULTIYEAR_BGC_004_011 (https://doi.org/10.48670/moi-00059) product for biogeochemistry, and NWSHELF_MULTIYEAR-_PHY-_004_009 (https://doi.org/10.48670/-moi-00058) for physics. We have used nitrate data-sets from the ICES portal (https://doi.org/10.17895/-ices.pub.8883), from the Western Channel Observatory (https://www.westernchannelobservatory.org.uk/l4_nutrients.php), and the Scottish Coastal Observatory (doi:10.7489/610-1, 10.7489/953-1, 10.7489/952-1, 10.7489/948-1, 10.7489/12138-1)

Author contributions. DSB wrote all the code, processed the data, developed the ML model and run the experiments. JS provided conceptualisation, supervision and funding acquisition. Both authors wrote the manuscript.

Competing interests. The authors declare that they have no conflict of interest.

Acknowledgements. This work was funded by the Horizon Europe project The New Copernicus Capability for Tropic Ocean Networks (NECCTON, grant agreement no.101081273). We also acknowledge support from the UK Natural Environment Research Council (NERC) single centre national capability programme – Climate Linked Atlantic Sector Science (CLASS, NE/R015953/1). The river data used here were prepared by Sonja van Leeuwen and Helen Powley as part of UK Shelf Sea Biogeochemistry programme (contract no.NE/K001876/1) of the NERC and the Department for Environment, Food and Rural Affairs (DEFRA). The riverine data contained also climatological values from the Global River Discharge Data Base and the Centre for Ecology and Hydrology (Young and Holt, 2007). We would like to thank Bee Berx for pointing us to the validation data from Scottish Coastal Stations. We would also like to thank Jerry Blackford, Gennadi Lessin, Yuri Artioli, Helen Powley, Julien Brajard and Dave Moffat for their valuable comments and discussions.

References

Anderson, D. M., Cembella, A. D., and Hallegraeff, G. M.: Progress in understanding harmful algal blooms: paradigm shifts and new technologies for research, monitoring, and management, Annual review of marine science, 4, 143–176, 2012.

Axe, P., Clausen, U., Leujak, W., Malcolm, S., and Harvey, E.: Eutrophication status of the OSPAR maritime area, Third Integrated Report on the Eutrophication Status of the OSPAR Maritime Area, 2017.

Axe, P., Sonesten, L., and Skarbövik, E.: Inputs of Nutrients to the OSPAR Maritime Area, 2022.

Baretta, J., Ebenhöh, W., and Ruardij, P.: The European regional seas ecosystem model, a complex marine ecosystem model, Netherlands Journal of Sea Research, 33, 233–246, 1995.

Behrenfeld, M. J. and Boss, E. S.: Resurrecting the ecological underpinnings of ocean plankton blooms, Annual review of marine science, 6, 167–194, 2014.

Beman, J. M., Popp, B. N., and Francis, C. A.: Molecular and biogeochemical evidence for ammonia oxidation by marine Crenarchaeota in the Gulf of California, The ISME Journal, 2, 429–441, 2008.

Board, O. S., Council, N. R., et al.: Clean coastal waters: understanding and reducing the effects of nutrient pollution, National Academies Press, 2000.

Borges, A., Schiettecatte, L.-S., Abril, G., Delille, B., and Gazeau, F.: Carbon dioxide in European coastal waters, Estuarine, Coastal and Shelf Science, 70, 375–387, 2006.

Bresnan, E., Cook, K., Hindson, J., Hughes, S., Lacaze, J., Walsham, P., Webster, L., and Turrell, W.: The Scottish coastal observatory 1997–2013. Part 2-description of Scotland's coastal waters, Scottish Marine and Freshwater Science, 7, 2016.

Brewin, R. J., Sathyendranath, S., Hirata, T., Lavender, S. J., Barciela, R. M., and Hardman-Mountford, N. J.: A three-component model of phytoplankton size class for the Atlantic Ocean, Ecological Modelling, 221, 1472–1483, 2010.

Brewin, R. J., Ciavatta, S., Sathyendranath, S., Jackson, T., Tilstone, G., Curran, K., Airs, R. L., Cummings, D., Brotas, V., Organelli, E., et al.: Uncertainty in ocean-color estimates of chlorophyll for phytoplankton groups, Frontiers in Marine Science, 4, 104, 2017.

Brockmann, U. and Eberlein, K.: River input of nutrients into the German Bight, in: The role of freshwater outflow in coastal marine ecosystems, pp. 231–240, Springer, 1986.

Brockmann, U., Topcu, D., Schütt, M., and Leujak, W.: Eutrophication assessment in the transit area German Bight (North Sea) 2006–2014– Stagnation and limitations, Marine pollution bulletin, 136, 68–78, 2018.

Bruggeman, J. and Bolding, K.: A general framework for aquatic biogeochemical models, Environmental modelling & software, 61, 249–265, 2014.

Burson, A., Stomp, M., Akil, L., Brussaard, C. P., and Huisman, J.: Unbalanced reduction of nutrient loads has created an offshore gradient from phosphorus to nitrogen limitation in the North Sea, Limnology and Oceanography, 61, 869–888, https://doi.org/10.1002/LNO.10257, 2016a.

Burson, A., Stomp, M., Akil, L., Brussaard, C. P., and Huisman, J.: Unbalanced reduction of nutrient loads has created an offshore gradient from phosphorus to nitrogen limitation in the N orth S ea, Limnology and Oceanography, 61, 869–888, 2016b.

Butenschön, M., Clark, J., Aldridge, J. N., Allen, J. I., Artioli, Y., Blackford, J., Bruggeman, J., Cazenave, P., Ciavatta, S., Kay, S., et al.: ERSEM 15.06: a generic model for marine biogeochemistry and the ecosystem dynamics of the lower trophic levels, Geoscientific Model Development, 9, 1293–1339, 2016.

Chen, S., Meng, Y., Lin, S., Yu, Y., and Xi, J.: Estimation of sea surface nitrate from space: Current status and future potential, Science of
    The Total Environment, p. 165690, 2023.

Devlin, M. J., Prins, T. C., Enserink, L., Leujak, W., Heyden, B., Axe, P. G., Ruiter, H., Blauw, A., Bresnan, E., Collingridge, K., et al.: A first
    ecological coherent assessment of eutrophication across the North-East Atlantic waters (2015–2020), Frontiers in Ocean Sustainability, 1,
    1253 923, 2023.

Diaz, R. J. and Rosenberg, R.: Spreading dead zones and consequences for marine ecosystems, science, 321, 926–929, 2008.

Doney, S. C., Fabry, V. J., Feely, R. A., and Kleypas, J. A.: Ocean acidification: the other CO2 problem, Annual review of marine science, 1,
    169–192, 2009.

Donlon, C. J., Martin, M., Stark, J., Roberts-Jones, J., Fiedler, E., and Wimmer, W.: The operational sea surface temperature and sea ice
    analysis (OSTIA) system, Remote Sensing of Environment, 116, 140–158, 2012.

Duarte, C. M.: Coastal eutrophication research: a new awareness, in: Eutrophication in Coastal Ecosystems: Towards better understanding
    and management strategies Selected Papers from the Second International Symposium on Research and Management of Eutrophication
    in Coastal Ecosystems, 20–23 June 2006, Nyborg, Denmark, pp. 263–269, Springer, 2009.

Duce, R. A., LaRoche, J., Altieri, K., Arrigo, K. R., Baker, A. R., Capone, D., Cornell, S., Dentener, F., Galloway, J., Ganeshram, R. S.,
    et al.: Impacts of atmospheric anthropogenic nitrogen on the open ocean, Science, 320, 893–897, 2008.

Durairaj, P., Sarangi, R. K., Ramalingam, S., Thirunavukarassu, T., and Chauhan, P.: Seasonal nitrate algorithms for nitrate retrieval using
    OCEANSAT-2 and MODIS-AQUA satellite data, Environmental Monitoring and Assessment, 187, 1–15, 2015.

Dutkiewicz, S., Follows, M., Marshall, J., and Gregg, W. W.: Interannual variability of phytoplankton abundances in the North Atlantic, Deep
    Sea Research Part II: topical studies in oceanography, 48, 2323–2344, 2001.

Follows, M. and Dutkiewicz, S.: Meteorological modulation of the North Atlantic spring bloom, Deep Sea Research Part II: Topical Studies
    in Oceanography, 49, 321–344, 2001.

Garcia, H., Weathers, K., Paver, C., Smolyar, I., Boyer, T., Locarnini, M., Zweng, M., Mishonov, A., Baranova, O., Seidov, D., et al.: World
    ocean atlas 2018. Vol. 4: Dissolved inorganic nutrients (phosphate, nitrate and nitrate+ nitrite, silicate), 2019.

Good, S., Fiedler, E., Mao, C., Martin, M. J., Maycock, A., Reid, R., Roberts-Jones, J., Searle, T., Waters, J., While, J., et al.: The current
    configuration of the OSTIA system for operational production of foundation sea surface temperature and ice concentration analyses,
    Remote Sensing, 12, 720, 2020.

Greenwood, N., Devlin, M. J., Best, M., Fronkova, L., Graves, C. A., Milligan, A., Barry, J., and Van Leeuwen, S. M.: Utilizing eutrophication
    assessment directives from transitional to marine systems in the Thames Estuary and Liverpool Bay, UK, Frontiers in Marine Science, 6,
    116, 2019.

Grosse, J., van Breugel, P., Brussaard, C. P., and Boschker, H. T.: A biosynthesis view on nutrient stress in coastal phytoplankton, Limnology
    and oceanography, 62, 490–506, 2017.

Harris, R.: The L4 time-series: the first 20 years, Journal of Plankton Research, 32, 577–583, 2010.

He, R., Chen, K., Fennel, K., Gawarkiewicz, G., and McGillicuddy Jr, D.: Seasonal and interannual variability of physical and biological
    dynamics at the shelfbreak front of the Middle Atlantic Bight: nutrient supply mechanisms, Biogeosciences, 8, 2935–2946, 2011.

Henson, S. A., Robinson, I., Allen, J. T., and Waniek, J. J.: Effect of meteorological conditions on interannual variability in timing and
    magnitude of the spring bloom in the Irminger Basin, North Atlantic, Deep Sea Research Part I: Oceanographic Research Papers, 53,
    1601–1615, 2006.

Hersbach, H., Bell, B., Berrisford, P., Hirahara, S., Horányi, A., Muñoz-Sabater, J., Nicolas, J., Peubey, C., Radu, R., Schepers, D., Simmons, A., Soci, C., Abdalla, S., Abellan, X., Balsamo, G., Bechtold, P., Biavati, G., Bidlot, J., Bonavita, M., Chiara, G. D., Dahlgren, P., Dee, D., Diamantakis, M., Dragani, R., Flemming, J., Forbes, R., Fuentes, M., Geer, A., Haimberger, L., Healy, S., Hogan, R. J., Hólm, E., Janisková, M., Keeley, S., Laloyaux, P., Lopez, P., Lupu, C., Radnoti, G., de Rosnay, P., Rozum, I., Vamborg, F., Villaume, S., and Thépaut, J. N.: The ERA5 global reanalysis, Quarterly Journal of the Royal Meteorological Society, 146, 1999–2049, https://doi.org/10.1002/QJ.3803, 2020.

Hill, R., Rinker, R., and Wilson, H. D.: Atmospheric nitrogen fixation by lightning, Journal of Atmospheric Sciences, 37, 179–192, 1980.

Hindson, J., Berx, B., Hughes, S., Walsham, P., Machairpoulou, M., Bresnan, E., and Turrell, B.: The Scottish Coastal Observatory, Bollettino di Geofisica, p. 333, 2018.

Hinrichs, I., Gouretski, V., Pätch, J., Emeis, K., and Stammer, D.: North sea biogeochemical climatology, 2017.

Huisman, J., van Oostveen, P., and Weissing, F. J.: Critical depth and critical turbulence: two different mechanisms for the development of phytoplankton blooms, Limnology and oceanography, 44, 1781–1787, 1999.

Huthnance, J. M., Holt, J. T., and Wakelin, S. L.: Deep ocean exchange with west-European shelf seas, Ocean Science, 5, 621–634, 2009.

Jahnke, R. A.: Global synthesis1, in: Carbon and nutrient fluxes in continental margins: A global synthesis, pp. 597–615, Springer, 2010.

Jin, H., Song, Q., and Hu, X.: Auto-keras: An efficient neural architecture search system, in: Proceedings of the 25th ACM SIGKDD international conference on knowledge discovery & data mining, pp. 1946–1956, 2019.

Kay, S., McEwan, R., and Ford, D.: North West European Shelf Production Centre NWSHELF_MULTIYEAR_BIO_004_011, CMEMS Report, 3, 21, 2016.

Lenhart, H.-J. and Große, F.: Assessing the effects of WFD nutrient reductions within an OSPAR frame using trans-boundary nutrient modeling, Frontiers in Marine Science, 5, 447, 2018.

Lenhart, H.-J., Mills, D. K., Baretta-Bekker, H., Van Leeuwen, S. M., Van Der Molen, J., Baretta, J. W., Blaas, M., Desmit, X., Kühn, W., Lacroix, G., et al.: Predicting the consequences of nutrient reduction on the eutrophication status of the North Sea, Journal of Marine Systems, 81, 148–170, 2010a.

Lenhart, H.-J., Mills, D. K., Baretta-Bekker, H., van Leeuwen, S. M., van der Molen, J., Baretta, J. W., Blaas, M., Desmit, X., Kühn, W., Lacroix, G., Los, H. J., Ménesguen, A., Neves, R., Proctor, R., Ruardij, P., Skogen, M. D., Vanhoutte-Brunier, A., Villars, M. T., and Wakelin, S. L.: Predicting the consequences of nutrient reduction on the eutrophication status of the North Sea, Journal of Marine Systems, 81, 148–170, https://doi.org/https://doi.org/10.1016/j.jmarsys.2009.12.014, contributions from Advances in Marine Ecosystem Modelling Research II 23-26 June 2008, Plymouth, UK, 2010b.

Loebl, M., Colijn, F., van Beusekom, J. E., Baretta-Bekker, J. G., Lancelot, C., Philippart, C. J., Rousseau, V., and Wiltshire, K. H.: Recent patterns in potential phytoplankton limitation along the Northwest European continental coast, Journal of Sea Research, 61, 34–43, 2009.

Madec, G., Bourdallé-Badie, R., Bouttier, P.-A., Bricaud, C., Bruciaferri, D., Calvert, D., Chanut, J., Clementi, E., Coward, A., Delrosso, D., et al.: NEMO ocean engine, 2017.

Nazari-Sharabian, M., Ahmad, S., and Karakouzian, M.: Climate change and eutrophication: a short review, Engineering, Technology and Applied Science Research, 8, 3668, 2018.

Noxon, J.: Atmospheric nitrogen fixation by lightning, Geophysical Research Letters, 3, 463–465, 1976.

OSPAR, C.: Common procedure for the identification of the eutrophication status of the OSPAR maritime area, OSPAR Commission, 3, 2005.

Painting, S., Van der Molen, J., Parker, E., Coughlan, C., Birchenough, S., Bolam, S., Aldridge, J., Forster, R., and Greenwood, N.: Development of indicators of ecosystem functioning in a temperate shelf sea: a combined fieldwork and modelling approach, Biogeochemistry, 113, 237–257, 2013.

Pauly, D., Christensen, V., Guénette, S., Pitcher, T. J., Sumaila, U. R., Walters, C. J., Watson, R., and Zeller, D.: Towards sustainability in world fisheries, Nature, 418, 689–695, 2002.

Philippart, C. J., Beukema, J. J., Cadée, G. C., Dekker, R., Goedhart, P. W., van Iperen, J. M., Leopold, M. F., and Herman, P. M.: Impacts of nutrient reduction on coastal communities, Ecosystems, 10, 96–119, 2007.

Postgate, J. R.: Nitrogen fixation, Cambridge University Press, 1998.

Rabalais, N. N., Turner, R. E., and Wiseman Jr, W. J.: Gulf of Mexico hypoxia, aka "The dead zone", Annual Review of ecology and Systematics, 33, 235–263, 2002.

Rabalais, N. N., Turner, R. E., Díaz, R. J., and Justić, D.: Global change and eutrophication of coastal waters, ICES Journal of Marine Science, 66, 1528–1537, 2009.

Radach, G.: Ecosystem functioning in the German Bight under continental nutrient inputs by rivers, Estuaries, 15, 477–496, 1992.

Radach, G. and Pätsch, J.: Variability of continental riverine freshwater and nutrient inputs into the North Sea for the years 1977–2000 and its consequences for the assessment of eutrophication, Estuaries and coasts, 30, 66–81, 2007.

Ryther, J. H. and Dunstan, W. M.: Nitrogen, phosphorus, and eutrophication in the coastal marine environment, Science, 171, 1008–1013, 1971.

Skákala, J., Ford, D., Brewin, R. J., McEwan, R., Kay, S., Taylor, B., de Mora, L., and Ciavatta, S.: The assimilation of phytoplankton functional types for operational forecasting in the northwest European shelf, Journal of Geophysical Research: Oceans, 123, 5230–5247, 2018.

Skákala, J., Ford, D., Bruggeman, J., Hull, T., Kaiser, J., King, R. R., Loveday, B., Palmer, M. R., Smyth, T., Williams, C. A., et al.: Towards a multi-platform assimilative system for North Sea biogeochemistry, Journal of Geophysical Research: Oceans, 126, e2020JC016 649, 2021.

Skákala, J., Bruggeman, J., Ford, D., Wakelin, S., Akpınar, A., Hull, T., Kaiser, J., Loveday, B. R., O'Dea, E., Williams, C. A., et al.: The impact of ocean biogeochemistry on physics and its consequences for modelling shelf seas, Ocean Modelling, 172, 101 976, 2022.

Skogen, M. D., Søiland, H., and Svendsen, E.: Effects of changing nutrient loads to the North Sea, Journal of Marine Systems, 46, 23–38, 2004.

Soetaert, K., Middelburg, J. J., Heip, C., Meire, P., Van Damme, S., and Maris, T.: Long-term change in dissolved inorganic nutrients in the heterotrophic Scheldt estuary (Belgium, The Netherlands), Limnology and oceanography, 51, 409–423, 2006.

Sonesten, L., Axe, P., Bellert, B., Burtschell, L., Eumont, D., Fairbank, V., Farkas, C., Graves, C., Martínez García-Denche, L., McDermott, G., Moeslund Svendsen, L., Mönnich, J., Nunes, S., Pohl, M., Posen, P., Sánchez Fernández, B., Skarbøvik, E., Thiesse, E., Vannevel, R., and Wilkes, R.: Waterborne and Atmospheric Inputs of Nutrients and Metals to the Sea. In: OSPAR, 2023: The 2023 Quality Status Report for the Northeast Atlantic, In: OSPAR, 2023: The 2023 Quality Status Report for the Northeast Atlantic. OSPAR Commission, London. Available at: https://oap.ospar.org/en/ospar-assessments/quality-status-reports/qsr-2023/other-assessments/inputs-nutrients-and-metals, 2022.

Sverdrup, H. U.: On conditions for the vernal blooming of phytoplankton, J. Cons. Int. Explor. Mer, 18, 287–295, 1953.

Tett, P., Droop, M. R., and Heaney, S. I.: The Redfield Ratio and Phytoplankton Growth Rate, Journal of the Marine Biological Association of the United Kingdom, 65, 487–504, https://doi.org/10.1017/S0025315400050566, 1985.

Topcu, D. and Brockmann, U.: Consistency of thresholds for eutrophication assessments, examples and recommendations, Environmental Monitoring and Assessment, 193, 1–15, 2021.

Ueyama, R. and Monger, B. C.: Wind-induced modulation of seasonal phytoplankton blooms in the North Atlantic derived from satellite observations, Limnology and Oceanography, 50, 1820–1829, 2005.

470 van Leeuwen, S. and Lenhart, H.: OSPAR ICG-EMO riverine database 2020-05-01 used in 2020 workshop, https://doi.org/10.25850/nioz/7b.b.vc, 2021.

Van Leeuwen, S. M., Lenhart, H.-J., Prins, T. C., Blauw, A., Desmit, X., Fernand, L., Friedland, R., Kerimoglu, O., Lacroix, G., Van Der Linden, A., et al.: Deriving pre-eutrophic conditions from an ensemble model approach for the North-West European seas, Frontiers in Marine Science, 10, 1129 951, 2023.

475 Voss, M., Bange, H. W., Dippner, J. W., Middelburg, J. J., Montoya, J. P., and Ward, B.: The marine nitrogen cycle: recent discoveries, uncertainties and the potential relevance of climate change, Philosophical Transactions of the Royal Society B: Biological Sciences, 368, 20130 121, 2013.

Withers, P. J., Neal, C., Jarvie, H. P., and Doody, D. G.: Agriculture and eutrophication: where do we go from here?, Sustainability, 6, 5853–5875, 2014.

480 Young, E. and Holt, J.: Prediction and analysis of long-term variability of temperature and salinity in the Irish Sea, Journal of Geophysical Research: Oceans, 112, 2007.

Yu, X., Chen, S., and Chai, F.: Remote estimation of sea surface nitrate in the California current system from satellite ocean color measurements, IEEE Transactions on Geoscience and Remote Sensing, 60, 1–17, 2021.

Zhai, L., Platt, T., Tang, C., Sathyendranath, S., and Walne, A.: The response of phytoplankton to climate variability associated with the
485 North Atlantic Oscillation, Deep Sea Research Part II: Topical Studies in Oceanography, 93, 159–168, 2013.